ELSEVIER

Journal of Chromatography A, 800 (1998) 135–150

JOURNAL OF CHROMATOGRAPHY A

Optimization strategy for simulated moving bed systems

Thomas Pröll[a,*], Ernst Küsters[b]

[a]*Pharma Engineering, Novartis Pharma Inc., 4002 Basel, Switzerland*
[b]*Chemical and Analytical Development, Novartis Pharma Inc., 4002 Basel, Switzerland*

Received 14 August 1997; received in revised form 4 November 1997; accepted 12 November 1997

Abstract

Simulated moving bed (SMB) systems are of rising interest in the purification of pharmaceuticals or specialty chemicals (racemic mixtures, proteins, organic acids, etc.). This is particularly due to their advantage in solvent reduction, obtained productivity and purities as well as investment costs in comparison to eluent chromatography. This paper evolved from the need for a readily available algorithm in order to find optimal operating conditions for SMB chromatography systems with nonlinear or coupled adsorption isotherms. The herein developed algorithm is based on a semi-deterministic two-step approach. First, optimal operating conditions with regard to an objective function are found by knowing adsorption measurements only. In a second step actual SMB results are used to adapt the initial isotherm measurements and match the simulation with the experiment. The algorithm is verified on a bench-scale SMB unit applied for the separation of a racemic epoxide with Chiralcel-OD as stationary phase. The developed algorithm improved the productivity of the investigated experimental design by 24%. © 1998 Elsevier Science B.V.

Keywords: Simulated moving bed; Adsorption isotherms; Enantiomer separation

1. Introduction

Simulated moving bed (SMB) chromatography has emerged as a promising technology for the separation of binary mixtures. The principle has already been commercialized under Universal Oil Products (UOP) some 30 years ago [1,2]. Since then the developed principle of SMB – for simulating a continuous counter-current operation to avoid the actual movement of the solid (''stationary'' phase) – has been applied very successful in several industries in very large scale (hydrocarbons, organic acids, sugars) [3]. Meanwhile, many examples deal with the resolution of racemates, which is becoming one of the major fields of application [4–9].

The SMB process works with the inherent advantage of a higher driving force because of the counter-current operation principle. Less solvent consumption, smaller apparatus scale, lower investment costs and higher yields are generally the results of this inherent advantage. In order to fully take advantage of this principle, a great number of operational parameters need to be adjusted properly – according to the given separation problem. An experimental evaluation of these operational parameters is very time consuming – a pseudo-stationary operation mode needs to be obtained first and long analytical procedures have to be applied – and is therefore quite costly.

In a series of papers Ching and Ruthven [10,11] developed the principles for modelling and simulating SMB systems in order to find internal profiles

*Corresponding author.

0021-9673/98/$19.00
PII S0021-9673(97)01146-1

and from those the optimal operational parameters. More recent experimental work has been reviewed by Ganetsos and Barker [12]. Due to the complexity in solving the modeling equations for the SMB system, the majority of the theoretical work has been focused on linear adsorption isotherms. Nonlinear and/or coupled adsorption isotherms (Langmuir type or other algebraic forms) are covered by Ching et al. [13] and Ruthven and Ching [14].

This paper introduces a two-stage procedure (optimization and adaptation) for finding proper operational parameters for a SMB system – especially designed for the case of nonlinear and/or coupled adsorption isotherms. The first stage – an optimization procedure – is based upon a multidimensional search algorithm. This optimization procedure finds the optimal operational parameters for a specific separation problem – stated by an objective function. The second stage is applied when experimental results of the SMB process are available. The main goal within the second stage is to find a match of the SMB simulation results with the SMB experimental results. This is accomplished by adapting the a priori measured adsorption isotherms until the match in the SMB results is accomplished. The experimental results of the SMB are given by the outlet concentration measurements.

Several techniques are described for measuring the adsorption isotherms, each of them having individual reasons for inaccuracy: errors in the determination of the bed voidage, errors in the analytical procedure for detecting the proper concentration and long equilibration times. The SMB measurements (outlet concentrations) are based upon a much more reliable procedure with longer operational times and more robust analytical techniques. The result is a smaller error potential and it shows the actual performance.

The overall goal of this work is to minimize the time and number of SMB experiments in order to achieve fast and accurate optimal operating conditions for a given separation problem. The paper briefly reviews the operational principle of SMB systems and the modelling principles as an equilibrium stage model. A link between the design equations for optimal operating conditions developed by Nicoud [15] and Ruthven and Ching [14] for linear adsorption systems is given.

Considering a linear design the developed two-stage algorithm is outlined. This algorithm is fully applicable for nonlinear and coupled adsorption isotherm systems as well, the algorithm is discussed in detail and flow charts for implementation are shown.

The experimental verification of the developed algorithm has been shown on a lab-scale in-laboratory developed SMB apparatus [7] operated in the SORBEX mode [2]. The separation problem consists of a racemic epoxide used extensively in the pharmaceutical development which has been chromatographed on the chiral stationary phase (CSP) Chiralcel-OD.

2. Concept of SMB

2.1. The SORBEX process

The concept of SMB as a continuous countercurrent process has extensively been reported in literature [14,16]. In this work the SMB system was considered to be operated in the SORBEX mode with four sections and four ports. An arbitrary example is given in Fig. 1. This mode of operation has shown to have advantages in solvent consumption as well as in the accuracy of simulation results compared to the three-section mode [17].

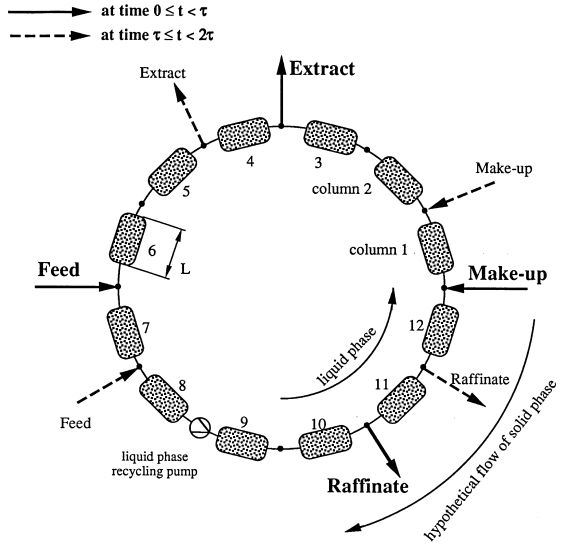

Fig. 1. Operational principle of an arbitrary SMB system.

Table 1
Definition of SMB sections

Section No.	Section placement
I	Between eluent and extract port
II	Between extract and feed port
III	Between feed and raffinate port
IV	Between raffinate and eluent port

The four sections are determined by the placement of the ports as given in Table 1. Switching the ports counter-clockwise (see Fig. 1) and pumping the mobile phase in the same direction leads to the counter-current simulated moving bed process represented in Fig. 2. The hypothetical constant solid-phase flow, $\dot{V}_S$, is from top to bottom, the counter-current fluid flow (mobile phase) from bottom to the top. Throughout the system four different liquid phase flow-rates occur – a different one for each section, $\dot{V}_{L,I}$ to $\dot{V}_{L,IV}$.

For modeling the SMB system, only the steady-state operation is considered. Because of the in-stationary port switching and flow-rate changes for each of the individual columns in one cycle, the steady-state operation represents an intermediate operation mode (quasi steady-state). However, for most practical purposes the stationary model is fully sufficient [10,16].

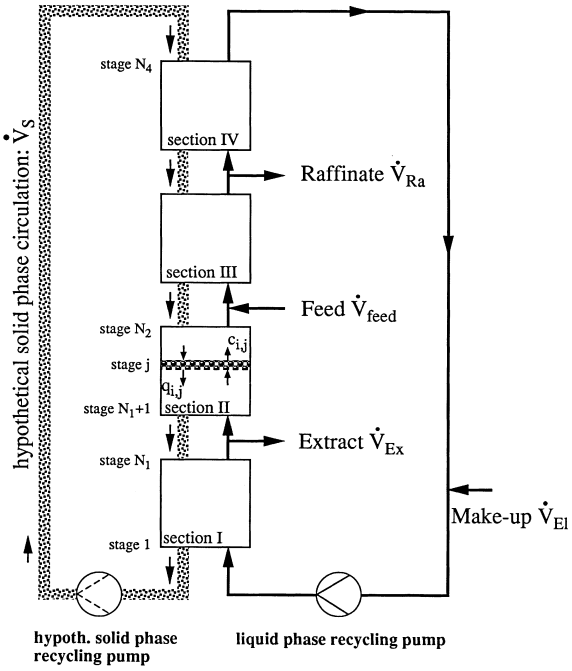

Fig. 2. The SMB model: a counter-current equilibrium stage process.

2.2. The equilibrium stage model

Basically, two methods are available in order to model the steady-state operation mode of the SMB process: (a) the plug flow reactor model – with or without axial dispersion – and (b) the equilibrium stage model that is represented by a series of continuous stirred tank reactors. Both models are related to each other by the concept of HETP (height equivalent of a theoretical plate) and should lead to the same results. In this work, focus has been given to the equilibrium stage model. Following the outline of Fig. 2, the constant solid-phase flow-rate throughout the system is

$$\dot{V}_S = (1-\varepsilon)Au \tag{1}$$

with ε as the overall bed voidage, A the column cross section and $u = L/\tau$ the effective solid velocity. Since the adsorption isotherms experimentally obtained are from the actual molecules which can not diffuse into the pores (the pores are filled and the particles are coated with the stationary phase), we assume that the obtained voidage is directly the bed voidage. τ represents the switching rate for one column and L is the length of one column. The effective liquid flow-rate, $\dot{V}_L$, is given in the SMB section m by

$$\dot{V}_{L,m} = \dot{V}'_{L,m} - V_C\frac{\varepsilon}{\tau} \tag{2}$$

with $\dot{V}'_{L,m}$ the actual (pumped) flow-rate in this section, and $V_C = LA$ as the column volume. $\dot{V}_{L,m}$ is also defined as the true moving bed liquid flow-rate (which is the flow available for the separation process) and $\dot{V}'_{L,m}$ as the simulated moving bed flow-rate.

Assuming no holdups and the total number of theoretical plates (all four sections) as N_4, the basic steady-state differential mass balance on stage j for component i is given as

$$\dot{V}_S(q_{i,j+1} - q_{i,j}) = \dot{V}_L(c_{i,j} - c_{i,j-1})$$
$$i = \text{A, B};\ j = 1....N_4 \tag{3}$$

with q as the solid-phase concentration, and c as the liquid phase concentration. $\dot{V}_L$ represents one of the four possible effective liquid flow-rates, $\dot{V}_{L,I}$ to $\dot{V}_{L,IV}$, depending on the section. Boundary conditions apply for the feed port stage (feed rate, $\dot{V}_{feed}$; concentration, $c_{i,feed}$) – Eq. (4) – and stage 0 – Eq. (5) [11].

$$c_{i,N_2[in]} = \frac{\left(c_{i,N_2[out]}\dot{V}_{L,II} + c_{i,feed}\dot{V}_{feed}\right)}{\dot{V}_{L,III}} \tag{4}$$

$$c_{i,0} = \frac{c_{i,N_4}\dot{V}_{L,IV}}{\dot{V}_{L,I}} \tag{5}$$

Introducing an arbitrary form of the distribution coefficient, K_i, by

$$K_i = K_{i[c_A,c_B]} \equiv \frac{q_i^*}{c_i}; \quad i = \text{A, B} \tag{6}$$

with q_i^* as the solid-phase equilibrium concentration, and assuming true equilibrium, the coupled nonlinear algebraic equation system

$$c_{A,j-1} - c_{A,j}\left[1 + \frac{\dot{V}_S}{\dot{V}_L}K_{A[c_{A,j};c_{B,j}]}\right] + c_{A,j+1}\frac{\dot{V}_S}{\dot{V}_L}K_{A[c_{A,j+1};c_{B,j+1}]} = 0$$

$$c_{B,j-1} - c_{B,j}\left[1 + \frac{\dot{V}_S}{\dot{V}_L}K_{B[c_{A,j};c_{B,j}]}\right] + c_{B,j+1}\frac{\dot{V}_S}{\dot{V}_L}K_{B[c_{A,j+1};c_{B,j+1}]} = 0$$

$$\text{with } j = 1....N_4 \text{ and } 0 \hat{=} N_4 \tag{7}$$

is obtained. Coupling of the set of Eq. (7) results only by assuming a cross-concentration dependency of the distribution coefficients given in Eq. (6).

3. Operational parameter design methods

3.1. Linear adsorption isotherms

The SMB system is exclusively a flow-controlled process by assuming linear adsorption isotherms. Nonlinear behavior of the isotherms adds to the dependency of the flow-rates the feed concentration as an influencing factor. Using the assumption of linear, uncoupled isotherms ($q_i = K_i c_i$), Nicoud [15] as well as Ching and Ruthven [18] give design equations for optimal operating conditions by introducing a common factor ξ. Nicoud [15] developed four constraints that consider proper levels of flow-rates in each one of the four SMB sections and pseudo-stationary concentration profiles within the system. These four constraints are represented by the following set of inequalities

$$\left[\dot{V}'_{L,I} - \dot{V}_S\frac{\varepsilon}{1-\varepsilon}\right]/\dot{V}_S > K_B \tag{8}$$

$$\left[\dot{V}'_{L,II} - \dot{V}_S\frac{\varepsilon}{1-\varepsilon}\right]/\dot{V}_S > K_A \tag{9}$$

$$\left[\dot{V}'_{L,III} - \dot{V}_S\frac{\varepsilon}{1-\varepsilon}\right]/\dot{V}_S < K_B \tag{10}$$

$$\left[\dot{V}'_{L,IV} - \dot{V}_S\frac{\varepsilon}{1-\varepsilon}\right]/\dot{V}_S < K_B \tag{11}$$

which can completely be solved for by incorporating a common factor $\xi >= 1.0$, by setting a feed flow-rate and using straightforward liquid flow mass balances around the ports of Fig. 2 [15]

$$\dot{V}_S = \dot{V}_{feed}\left\{\left[\frac{\varepsilon}{1-\varepsilon} + K_B\right]\frac{1}{\xi} - \left[\frac{\varepsilon}{1-\varepsilon} + K_A\right]\xi\right\}^{-1} \tag{12}$$

$$\dot{V}_{rec} = \dot{V}'_{L,I} = \xi\dot{V}_S\left[\frac{\varepsilon}{1-\varepsilon} + K_B\right] \tag{13}$$

$$\dot{V}_{Ex} = \xi\dot{V}_S(K_B - K_A) \tag{14}$$

$$\dot{V}_{Ra} = \frac{\dot{V}_S}{\xi}(K_B - K_A) \tag{15}$$

ξ has a theoretical limit of $\xi \leq \{[K_B + \varepsilon/(1+\varepsilon)]/[K_A + \varepsilon/(1-\varepsilon)]\}^{0.5}$ but in general a much lower practical limit is given due to a maximum pressure drop ($\xi = 1.0$ represents a minimum dilution and an increasing amount of solvent is given for $\xi > 1$). The equivalent design of Ching and Ruthven [18] is obtained by introducing the flow velocities $v' = \dot{V}'_L/(\varepsilon A)$, $v = \dot{V}_L/(\varepsilon A)$ and applying Eqs. (1) and (2) on the first constraint of Nicoud [15] (Eq. (8)) which gives

$$\frac{\varepsilon v_I}{(1-\varepsilon)u} > K_B \tag{16}$$

Rearranging of Eq. (16) gives

$$K_B \frac{(1-\varepsilon)}{\varepsilon} \frac{u}{v_I} < 1 \quad (17)$$

which is equivalent to the definition of the dimensionless separation factor, γ, from Ching and Ruthven [18]

$$\gamma_{B,I} = K_B \frac{(1-\varepsilon)}{\varepsilon} \frac{u}{v_I} < 1 \quad (18)$$

Both designs lead to the required net flow directions of the adsorbents in the four SMB sections outlined in Table 2 by means of the dimensionless separation factor.

The purities for a specific separation can be obtained by solving for the $2N_4$ unknowns of Eq. (7) ($c_{i,j}$; $\forall i$ = A, B; $j = 1....N_4$) with the flow-rates obtained from the previous optimal linear design approach. The concentration profile within the SMB system and therefore the purities are independent of the feed concentrations.

This linear adsorption design method will only give satisfactory results for adsorption isotherms that show even for larger concentration ranges a linear behavior. Because of the fact that within the SMB system large variations in concentration occur and many practically important separation problems do not conform to the linear adsorption model, the resulting design Eqs. (12)–(15) are only applicable for limited cases. However, the required net flow directions as outlined in Eqs. (8)–(11) and in Table 2 still remain valid even for the nonlinear case.

3.2. Nonlinear adsorption isotherms

3.2.1. Objective function

Assuming nonlinear concentration dependency of the adsorption behavior – according to the general Eq. (6) – the dimensionless separation factor γ as well as the constraints of Eqs. (8)–(11) do not remain constant within a section as it is the case for a linear adsorption isotherm. This results from the different separation behavior at each stage due to the concentration dependency of the distribution coefficients. Due to this dependency no explicit design for optimal operating conditions is available. Additionally, the pseudo steady-state concentration profile within the SMB system (which influences the obtained purities at the exit ports) depends on the feed concentration. The feed concentration represents for the nonlinear case an additional design parameter.

Table 2
Required separation factors (A...less adsorbing enantiomer, B...stronger adsorbing enantiomer)

Section No.	γ_A	γ_B
I	<1	<1
II	<1	>1
III	<1	>1
IV	>1	>1

Depending on the given separation problem and its objective (e.g., maximum productivity of only one component, or of both components; or combinations thereof) a specific objective function, J, can be defined. Such an objective function would be for the case of maximum total amount of enantiomer purified per time of the following form

$$\max_{\dot{V}_{feed},\, c_{feed},\, \tau,\, \dot{V}_{Ex},\, \dot{V}_{Ra},\, \dot{V}_{rec}} J = \dot{V}_{Ra}(\text{e.e.}_{A,Ra}) c_{A,Ra} + \dot{V}_{Ex}(\text{e.e.}_{B,Ex}) c_{B,Ex} \quad (19)$$

Eq. (19) represents a commonly used objective in the separation of racemic mixtures, where only the separated portion is of interest

$$\text{e.e.}_{A,Ra} \equiv \frac{(c_{A,Ra} - c_{B,Ra})}{(c_{A,Ra} + c_{B,Ra})} \cdot 100 \quad (20)$$

where $\text{e.e.}_{A,Ra}$ represents the enantiomer excess of A in the raffinate stream (in percent). If the eluent consumption is of interest as well and should be kept low, the objective function of Eq. (19) can be altered by adding an additional term

$$\max_{\dot{V}_{feed},\, c_{feed},\, \tau,\, \dot{V}_{Ex},\, \dot{V}_{Ra},\, \dot{V}_{rec}} J^* = \Omega_1 J - \Omega_2 (\dot{V}_{feed} + \dot{V}_{Eluent}) \quad (21)$$

and using appropriate weighing values Ω_1 and Ω_2. All possible objective functions use the same decision variables, $\dot{V}_{feed}$, c_{feed}, τ, $\dot{V}_{Ex}$, $\dot{V}_{Ra}$ and $\dot{V}_{rec}$.

As for the linear case, $\dot{V}_{rec}$, has a practicable limit due to the maximum allowable pressure drop within one section. A good choice would be a design with a

value for the recycling flow just below the allowable pressure drop. All other decision variables need to be determined by an optimization procedure.

A two-step methodology is presented in order to solve this optimization problem efficiently. The first step assumes the availability of the adsorption isotherms from experiments (nonlinear and/or coupled), the second step additionally incorporates actual experimental SMB results (concentrations of the outlet streams). Both steps are designed to achieve with a minimum number of SMB experiments optimal operational parameters according to a given separation problem and objective function.

3.2.2. Initial design

This first step is based on the knowledge of the adsorption isotherms (adsorption measurements) but no experimental SMB result is present. Because of the varying concentrations within a SMB system, the adsorption isotherms need to be obtained for several concentrations and concentration mixtures – which can be a tedious and time consuming exercise. Practically only a few selections of the expected concentration variations and mixtures can be chosen and, therefore, limited information is available. Appropriate adsorption models, such as the Langmuir or Freundlich model or any other arbitrary structure that is best suited is used to fit the experimental data points.

These initial structures represent the initial models of the adsorption isotherms that are used for the first step in the design of optimal operating conditions. Table 3 shows the algorithm used for finding the optimal decision variables, $\boldsymbol{y}^* = \left[\dot{V}_{\text{feed}}, c_{\text{feed}}, \tau, \dot{V}_{\text{Ex}}, \dot{V}_{\text{Ra}}, \dot{V}_{\text{rec}}\right]^T$. The algorithm is based upon a straightforward Newton search method which generates its search direction, **s**, by

$$\mathbf{s} = -\mathbf{H}_y^{-1} \nabla J_y \tag{22}$$

by means of the Hessian matrix, $\mathbf{H}_y$,

$$\mathbf{H}_y = \nabla^2 J_y = \begin{bmatrix} \dfrac{\partial^2 J}{\partial \dot{V}_{\text{feed}}^2} & \cdots & \dfrac{\partial^2 J}{\partial \dot{V}_{\text{feed}} \partial \dot{V}_{\text{rec}}} \\ \vdots & & \vdots \\ \dfrac{\partial^2 J}{\partial \dot{V}_{\text{rec}} \partial \dot{V}_{\text{feed}}} & \cdots & \dfrac{\partial^2 J}{\partial \dot{V}_{\text{rec}}^2} \end{bmatrix} \tag{23}$$

and the gradient vector, ∇J_y,

$$\nabla J_y = \left[\frac{\partial J}{\partial \dot{V}_{\text{feed}}}, \frac{\partial J}{\partial c_{\text{feed}}}, \ldots \frac{\partial J}{\partial \dot{V}_{\text{rec}}} \right]^T \tag{24}$$

Faster converging or local minima avoiding algorithms (Broyden, Fletcher, Goldfarb and Shanno procedure or modified Marquardt algorithm) may also be applied [19–21]. Since this optimization problem does not have to converge within a real-time application, the less powerful Newton search is fully applicable. The elements of $\mathbf{H}_y$ and ∇J_y are calculated by a central difference method, and η_1 of Table 3 represents a predefined stopping criterion.

The initialization of Table 3 is done by a priori estimates for $\dot{V}_{\text{feed}}$ and c_{feed} (e.g., from linear estimates or adsorption experiments). The setting of $\xi = 1.05$ is in accordance with findings from Nicoud [15] and k represents the iteration interval.

The result of Table 3 is vector $\mathbf{y}^*$, which represents the optimal decision values for maximizing J (Eq. (21)). All applicable limitations on the elements of $\mathbf{y}^k$ need to be verified before a new profile is being calculated.

Some of the generally occurring limitations are due to the maximum allowable liquid flow-rate, the maximum feed concentration to which the adsorption model is accurate, a minimum switching time for obtaining quasi-steady-state operation and non-negative concentration and flow values.

With the obtained optimal decision vector $\mathbf{y}^*$ an initial SMB experiment has to be performed for verifying the simulation results. In the following second design step, such measured SMB results will be incorporated into the optimization procedure.

3.2.3. Design by incorporation of experimental SMB data

Adsorption measurement methods – even accurate ones – are not satisfactory for the application in SMB systems. The main drawbacks are given by (i) strongly varying concentrations of each of the components within a SMB unit, (ii) strongly varying concentration ratios of the components within a SMB unit, (iii) concentration fluctuations due to port switching and (iv) non-homogeneous adsorption behavior of the individual columns.

These difficulties generally cause deviations of the

Table 3
Algorithm for finding optimal operating conditions for a given SMB objective function

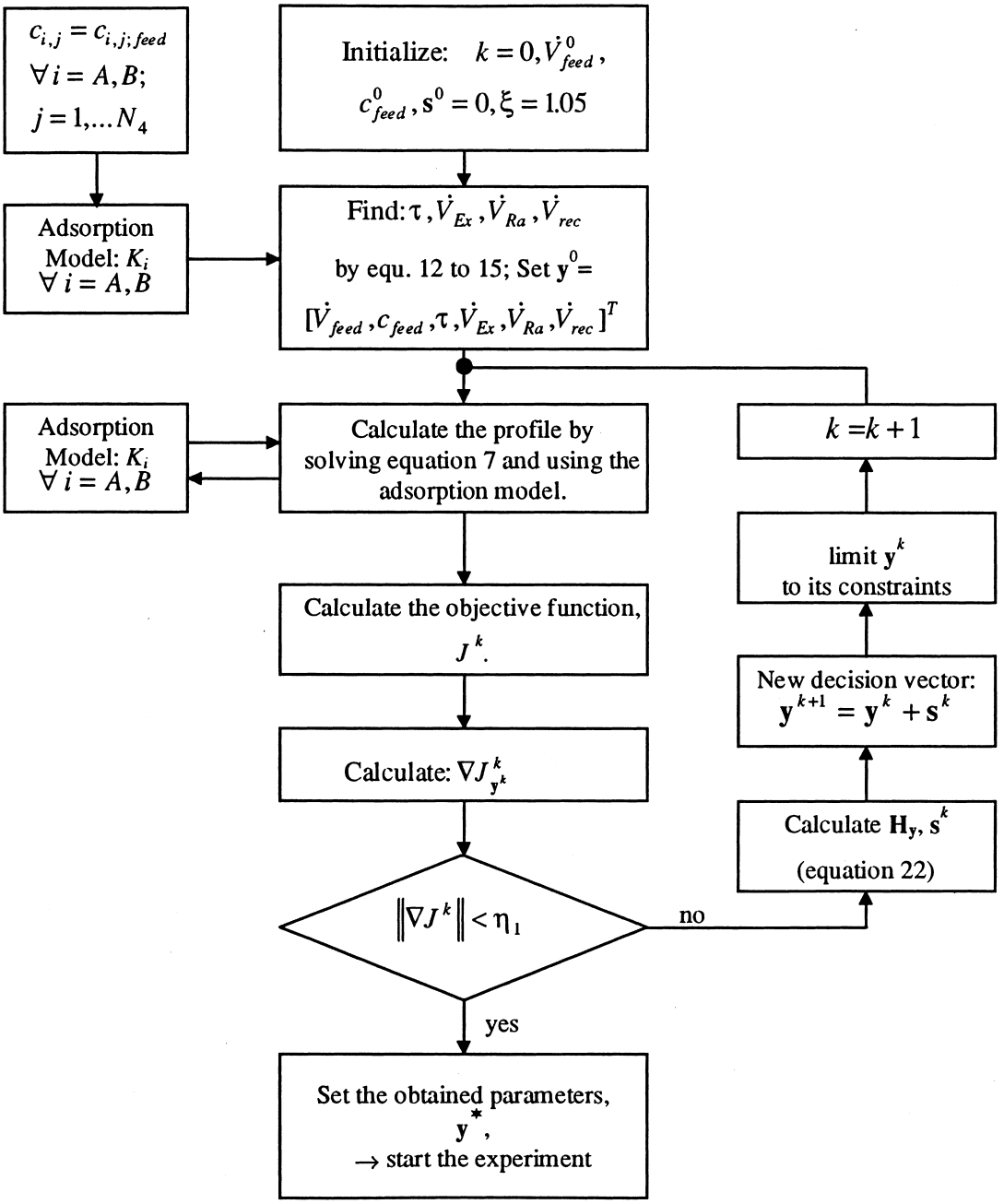

actually occurring adsorption from the measured adsorption isotherms. Only some of the above insufficiencies could be compensated by performing a wide range of adsorption measurements. The non-homogeneous behavior of the columns and the quasi-steady-state behavior due to the port switching still remains.

By performing an actual SMB run, experimental data of the internal profile can be obtained – either by measuring the concentrations on the outlet ports only or from additional sample ports between the individual columns. These concentration measurements are considered to be very accurate representations of the system behavior (long sampling times and accurate concentration determination methods). The port concentrations can be used to obtain information about the internal profile of the SMB system and to obtain information about the steady-state behavior of the process.

The estimated concentrations by simulation at the outlet ports ($\hat{c}_{i,\mathrm{Ex}}$, $\hat{c}_{i,\mathrm{RA}}$; $\forall i = \mathrm{A, B}$), and the concentrations measured from the experiment ($c_{i,\mathrm{Ex}}$, $c_{i,\mathrm{RA}}$; $\forall i = \mathrm{A, B}$), are compared and an error vector is defined

$$\boldsymbol{e}_l = \left[(c_{\mathrm{A},l} - \hat{c}_{\mathrm{A},l}), (c_{\mathrm{B},l} - \hat{c}_{\mathrm{B},l}) \right]^T \quad l = \mathrm{Ex, Ra} \qquad (25)$$

By means of this error vector the adsorption isotherm model of Eq. (6) can be corrected following the semi-deterministic procedure of Table 4.

Step a of the correction procedure of Table 4 can be performed by means of a deterministic search algorithm (first- or second-order [19]). For steps b and c no automated deterministic design is possible, an exhaustive search in form of a heuristic update of the structure needs to be performed. No a priori definition of the change of the concentration profiles in accordance to a change in the isotherm structure can be given. Therefore, this exhaustive search is implemented. It is mainly up to the user to find appropriate adsorption model structures that match the experimental data once step a of the algorithm in Table 4 is not sufficient. It is of advantage to start by adding single terms such as linear coupling (see Table 4) or continuous functions with well-defined behavior [e.g.,: $1 - \exp(-K_{\mathrm{A}_3} c_{\mathrm{B}})$). Table 5 shows the overall outline of the algorithm in order to match the simulation results with the SMB experiments.

Once a satisfactory correction for the adsorption model is found by the algorithm outlined in Table 5, this corrected model is reapplied in the optimization algorithm as outlined in Table 3. A new optimal design $\mathbf{y}^*$ is found, a new SMB experiment is performed and the correction of Table 5 starts again.

These iterations between the algorithms of Tables 3 and 5 minimize the number of very time consuming SMB experiments by proper incorporating modeling and simulation and lead efficiently to the desired optimal operating conditions. Avoiding even a single SMB result during the search for optimal conditions may result in substantial time savings (due to the time an experimental system reaches a quasi-steady-state and analytical procedures, etc.).

4. Results

4.1. Materials and methods

All equipment details of the SMB system used for generating the experimental results have been published in a previous paper [7] and are summarized in Table 6.

All columns were slurry packed (15 g CSP/200 ml mobile phase) for 10 min at 100 bar and tested individually. The retention times of the test racemate, specified below, on these columns were within 2% of each other as can be seen from Table 7. Validation experiments, to determine the upper limit of the

Table 4
Semi-deterministic three step procedure to correct the adsorption isotherm model

Step	What to do
a	Correct the coefficients of the initial model (i.e.,: K_{A_0}, K_{A_1}, etc.)
b	Add nonlinear terms of the same constituent to a linear model (i.e.,: $K_{\mathrm{A}} = K_{\mathrm{A}_0} + K_{\mathrm{A}_1} c_{\mathrm{A}} + K_{\mathrm{A}_2} c_{\mathrm{A}}^2$)
c	Add linear or nonlinear terms of a different constituent (i.e.,: $K_{\mathrm{A}} = K_{\mathrm{A}_0} + K_{\mathrm{A}_1} c_{\mathrm{A}} + K_{\mathrm{A}_2} c_{\mathrm{A}}^2 + K_{\mathrm{A}_3} c_{\mathrm{B}}$)

Table 5
Heuristic model adaptation algorithm for SMB system

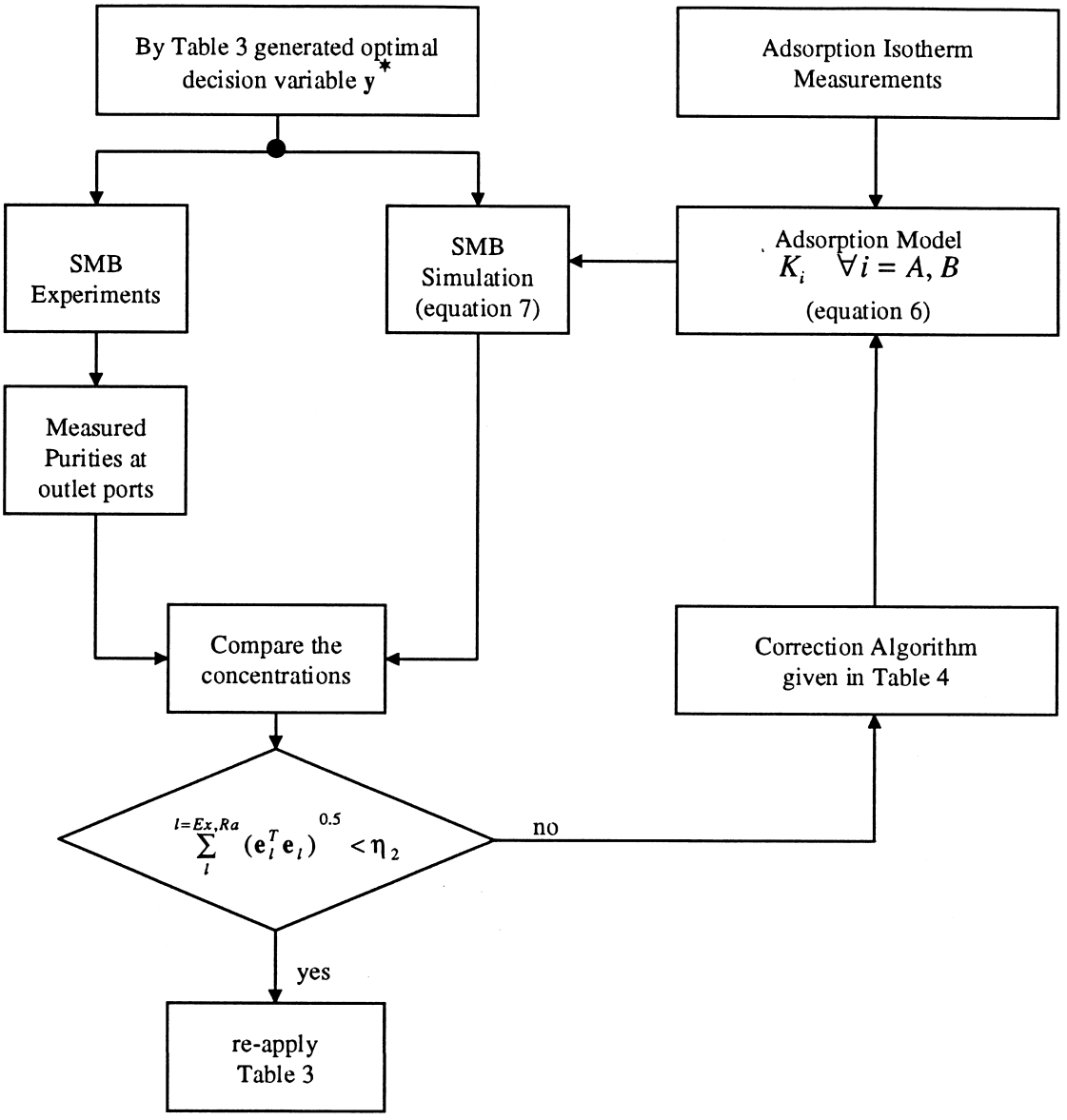

standard deviation, have so far not been conducted. The number of plates for each enantiomer is typically between 2000 and 2500.

The experimental problem is defined by the separation of 1*a*,2,7,7*a*-tetrahydro-3-methoxynaphth-(2,3*b*)-oxirene (CAS No.: 103009-62-7) that is used enantiomerically pure in kilogram quantities. Enantiomeric excess of raffinate and extract were determined on an analytical Chiralcel-OD column (25 cm length and 4 mm I.D.) using hexane–isopropanol (9:1) as mobile phase and a flow-rate of 0.5 ml/min ($K_B = 2.4$, $K_A = 1.63$).

Table 6
Experimental SMB system

Total No. of columns: 12	Mobile phase: hexane–isopropanol (9:1)
Columns per section: 3	Packing method: slurry
Column volume: 20.1 ml ($L=10$ cm, I.D.$=1.6$ cm)	Pumps: Jasco (remote controlled)
Stationary phase: Chiralcel-OD (Daicel)	Valves: 4 VICI (12-port each)
Control of switching cycles, pump rates: PC based	No. of stages per column: 13

Two objective functions have been chosen. One for the total amount purified per minute, J_1, (Eq. (19)) and the second one for the percentage of the total feed stream purified (conversion):

$$J_2 = \frac{J_1}{\dot{V}_{\text{feed}}(c_{\text{A,feed}} + c_{\text{B,feed}})} \tag{26}$$

All simulation results have been generated by using an in-laboratory available VAX-Cluster and a suitable subroutine for the set of nonlinear algebraic equations [22].

4.2. Adsorption isotherm measurements

Two methods have been used for obtaining the functionality of the adsorption process over the expected concentration and concentration ratio range within the SMB system. At low racemic concentrations (less than 0.25 g/l) breakthrough curves on a single column (equivalent to the SMB columns) were obtained. The flow-rate of $\dot{V}_{\text{feed}}=3$ ml/min was chosen within the range of the actually used ones (a maximum flow-rate of 4.0 ml/min was given due to the pressure drop). A zero retention time of $t_0=4.5$ min and pure component retention times of $t_A=11.7$ min and $t_B=16.0$ min was given for the (external) porosity, ε,

$$\varepsilon = \frac{V_{\text{mobile phase}}}{V_C} = \frac{t_0 \dot{V}_{\text{feed}}}{V_C} = 0.67 \tag{27}$$

and for the linear distribution coefficients,

$$K_i = \frac{t_i - t_0}{t_0} \frac{\varepsilon}{1-\varepsilon} \quad \forall i = \text{A, B} \tag{28}$$

$K_A=3.27$ and $K_B=5.22$. For higher concentrations frontal chromatography experiments on the pure components as well as racemic mixtures were applied. Using the same single column as for the break through measurements and the same flow-rate a feed with known concentrations, $c_{i,\text{feed}}$, was pumped

Table 7
Chromatographic data for the enantioseparation of our epoxide on each SMB column

Column No.	$t_{(+)}$ (min)	$t_{(-)}$ (min)	$k'_{(+)}$	$k'_{(-)}$	α
1	11.90	15.85	1.68	2.57	1.53
2	12.02	16.23	1.71	2.66	1.56
3	12.25	16.53	1.76	2.72	1.55
4	11.89	15.99	1.68	2.60	1.55
5	11.95	15.86	1.69	2.57	1.52
6	11.93	16.09	1.69	2.62	1.56
7	11.87	15.97	1.67	2.60	1.55
8	11.98	16.14	1.70	2.64	1.55
9	11.86	15.90	1.67	2.58	1.54
10	11.69	15.72	1.63	2.54	1.56
11	11.70	15.66	1.64	2.53	1.55
12	11.85	15.67	1.67	2.53	1.52
Mean	11.91	15.97	1.68	2.60	1.55
S.D. (%)	1.23	1.56	1.96	2.19	0.71

Chromatographic parameters: mobile phase: hexane–isopropanol (9:1, v/v), 3.0 ml/min; UV detection: 225 nm; injection amount: 0.2 mg.

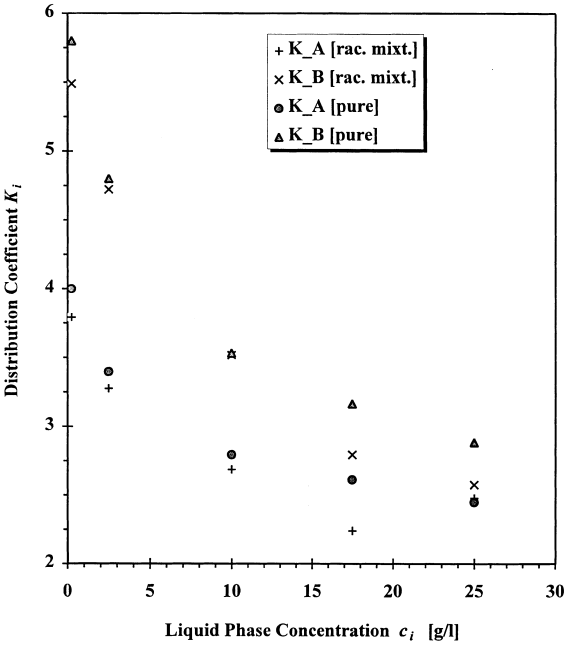

Fig. 3. Adsorption isotherm measurements based on breakthrough curves and frontal chromatography experiments.

through the column until equilibrium with the stationary phase has been achieved, q_i. By switching the feed to pure eluent, collecting and analyzing the washed-out regenerate, the equilibrium concentration of the stationary phase is obtained by

$$q_i^* = \frac{M_i - \varepsilon V_C c_{i,\text{feed}}}{(1-\varepsilon)V_C} \quad \forall i = \text{A, B} \tag{29}$$

with M_i as the overall amount of component i collected. Measurements have been obtained for racemic mixtures as well as for the pure components at 2.5, 12.5, 17.5 and 25 g/l per isomer. Fig. 3 shows the distribution coefficients for the low concentration measurements (breakthrough method) and for the higher concentrations (frontal analysis). Both isomers show a strong concentration dependency.

4.3. Preliminary SMB results

In order to verify the strong concentration dependencies of the distribution coefficients as obtained from the adsorption measurements a series of four SMB experiments were performed. This series of experiments is not necessary for the optimization procedure but illustrates the influence of the feed concentrations on the purification results and therefore on the concentration dependency of the adsorption.

Experimental runs 01 and 02 were performed with exactly the same flow-rates but at different feed concentrations, similar setup is valid for the runs 03 and 04 as given in Table 8.

The operational parameters for these experiments were obtained by an initial application of the algorithm of Table 2 – with the linear distribution coefficients. Experimental runs 01 and 02 were evaluated over more than 28 cycles (4300 min), experiments 03 and 04 for more than 12 cycles (1870 min). The results are given in Table 9.

Table 9 states the influence of the concentration on the obtained SMB results, which itself is influenced by concentration dependent changes in the adsorption behavior. In case of linear adsorption isotherms, experimental runs 01 and 02 would result in similar enantiomer excess (e.e.) and J_2 values, and the yield would have to be in correlation to the feed concentrations. Similar is applicable to run 03 and 04.

4.4. Optimal design using proposed methodology

4.4.1. Matching experimental data

Before an optimal design can actually be started, a

Table 8
Operational parameters for preliminary SMB experiments

Run No.	$C_{i,\text{feed}}$ (g/l)	$\dot{V}'_{\text{feed}}$ (ml/min)	$\dot{V}'_{\text{L,I}}$ (ml/min)	$\dot{V}'_{\text{L,II}}$ (ml/min)	$\dot{V}'_{\text{L,III}}$ (ml/min)	$\dot{V}'_{\text{L,IV}}$ (ml/min)	$\dot{V}_{\text{S}}$ (ml/min)
01	0.25	0.6	3.84	2.84	3.44	2.44	0.51
02	2.5	0.6	3.84	2.84	3.44	2.44	0.51
03	10	0.4	3.84	2.64	3.04	2.24	0.51
04	15	0.4	3.84	2.64	3.04	2.24	0.51

Table 9
Results for preliminary SMB experiments

Run No.	Raffinate		Extract		Performance	
	Yield (mg/min)	e.e.$_A$ (%)	Yield (mg/min)	e.e.$_B$ (%)	J_1 (mg/min)	J_2 (%)
01	0.13	73.3	0.17	62.6	0.169	56
02	1.49	96.5	1.51	98.2	2.882	96
03	3.98	95.0	4.02	94.4	7.375	92
04	7.93	55.2	4.07	95.4	7.269	60

suitable adsorption model needs to be found. This search has been conducted in accordance to the developed semi-deterministic algorithm of Tables 4 and 5. For the linear design, the adsorption model has been chosen according the breakthrough measurements: case a: $K_A=3.27$; $K_B=5.22$.

A nonlinear decoupled structure that fits the experimental isotherm data well was found by an exhaustive search: case b: $K_A=3.972-0.145c_A+0.004c_A^2$ and $K_A=2.478$ for $c_A>18.0$ (g/l); $K_B=5.300-0.237c_B+0.005c_B^2$ and $K_B=2.479$ for $c_B>23.5$ (g/l).

Even this optimized nonlinear, decoupled structure could not match the experimental SMB data satisfactorily as given in Table 10. An additional coupling term needed to be introduced which lowered the distribution coefficient for the weaker adsorbing constituent (A) in dependence of the concentration of the stronger adsorbing constituent (B): case c: $K_A=3.242-0.145c_A+0.004c_A^2+0.01c_B+0.65\ \exp(-c_B)$ and $K_A=2.478$ for $c_A>18.0$ (g/l); K_B remains the same as for the nonlinear, decoupled case.

Table 10 shows the mismatch in the exit port concentrations by using linear and nonlinear adsorption isotherms – even though the model isotherms accurately match the experimental adsorption measurements. Only the introduction of a coupling term for higher concentrations of A gives satisfactory results. The fit of the adsorption models (case b and case c) are given in Fig. 4 – by showing the distribution coefficients for the pure components. Fig. 5 shows the selectivity, $S=K_B/K_A$ as a function of c_A and c_B for case c.

An optimum selectivity for this model is at low concentrations of B ($c_B<3$ g/l) and high concentrations of A ($c_A>12$ g/l). A reverse of elution seems obtainable at low concentrations of A and high concentrations of B ($c_A<6$ g/l, $c_B>18$ g/l) which is in general not an uncommon observation [23]. An experimental verification is difficult to perform since the solubility of pure enantiomers is 25 g/l. Figs. 6 and 7 show the calculated profiles for run 03, with the assumption of linear distribution coefficient (case a) and nonlinear, coupled distribu-

Table 10
Comparison of experimental and simulated SMB results

Run No.	Exp. results		Simulation case a		Simulation case b		Simulation case c	
	Raffinate	Extract	Raffinate	Extract	Raffinate	Extract	Raffinate	Extract
Yield (mg/min)								
01	0.13	0.17	0.15	0.15	0.13	0.17	0.13	0.17
02	1.49	1.51	1.52	1.48	1.45	1.55	1.55	1.45
03	3.98	4.02	3.34	4.66	3.67	4.33	3.93	4.05
04	7.93	4.07	5.01	6.99	6.83	5.17	7.53	4.44
Purity (% e.e.)								
01	73.3	62.6	96.4	98.8	86.3	60.3	74.2	60.1
02	96.5	98.2	96.4	98.8	92.0	86.2	92.7	98.9
03	95.0	94.4	98.0	70.3	96.8	82.2	98.8	95.2
04	55.2	95.4	98.0	70.3	64.2	84.7	54.9	95.0

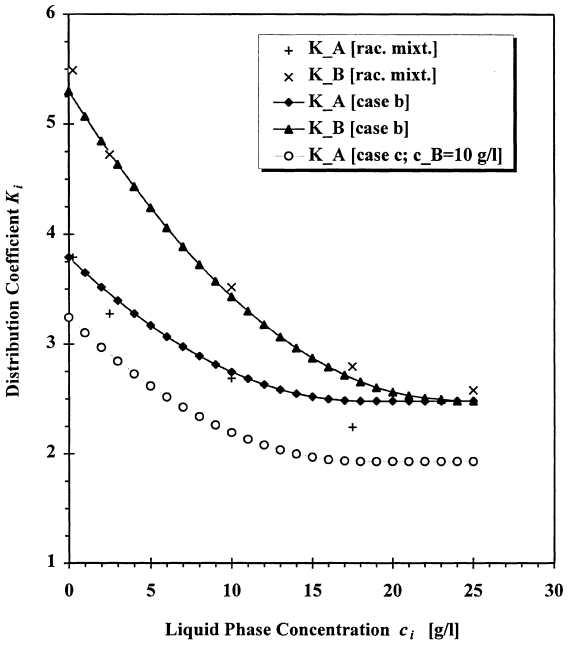

Fig. 4. Adsorption isotherm models: nonlinear and nonlinear coupled.

tion coefficients (case c), respectively. Fig. 6a and Fig. 7a show the dimensionless separation coefficients γ_A and γ_B as well as the purities. Fig. 6b and Fig. 7b give the actual profile.

4.4.2. Optimal design

The best result of the preliminary SMB experiments was run 03 ($J_1 = 7.375$ mg/min) which could not be improved based on experimental experience – even by several additional experiments. The problem was – as already outlined – the large number of decision variables. Applying the algorithm shown in Table 3 with the distribution coefficients of case c (nonlinear, coupled), an optimal design was searched for. The design was based on the objective function given in Eq. (19) and a maximum recycling rate of $\dot{V}_{rec} = 4.0$ ml/min. The search for (bounded) optimal decision variables gives the settings of Table 11.

Table 12 shows the calculated purities (outlet ports) and the actual values analyzed from the experimental SMB run, Fig. 8 shows the separation coefficients and the simulated internal profile.

From numerous simulations a sensitivity of the decision variables on the purities and the yield could

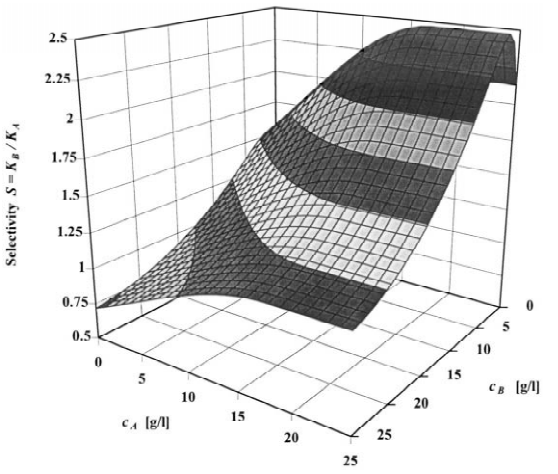

Fig. 5. Selectivity as a function of c_A and c_B.

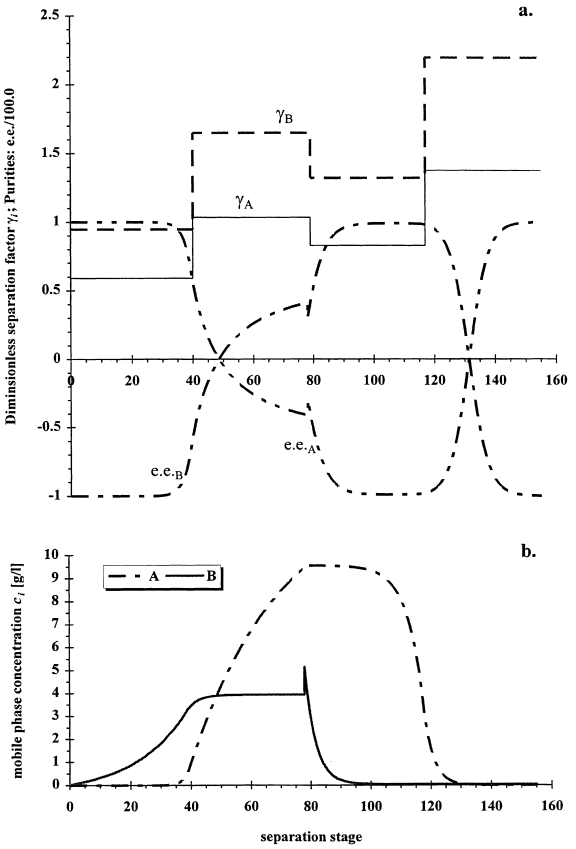

Fig. 6. (a) Dimensionless separation factor and purities for the linear adsorption case. (b) Concentration profile within the SMB system.

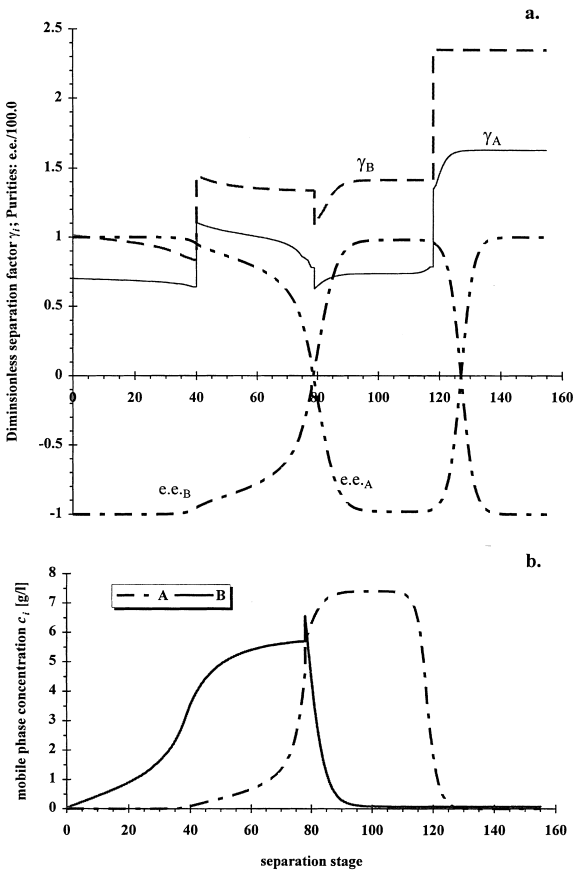

Fig. 7. (a) Dimensionless separation factor and purities for the nonlinear coupled adsorption case. (b) Concentration profile within the SMB system.

be obtained. The solid-phase flow-rate of $\dot{V}_S = 0.51$ ml/min is equivalent to a switching time of $\tau = 12.3$ min. Increasing the switching time (slower solid-phase flow-rate) to 13 min results in a drop of the raffinate enantiomer excess to e.e.$_A < 50\%$. Also the feed concentration shows a very strong dependency.

Table 12
Comparison of the simulated and experimental results for the optimized design

Run No.	Raffinate e.e.$_A$ (%)	Extract e.e.$_B$ (%)	J_1 (mg/min)	J_2 (%)
Opt. Sim.	98	91	9.716	92
Opt. Exp.	85	97	9.145	87

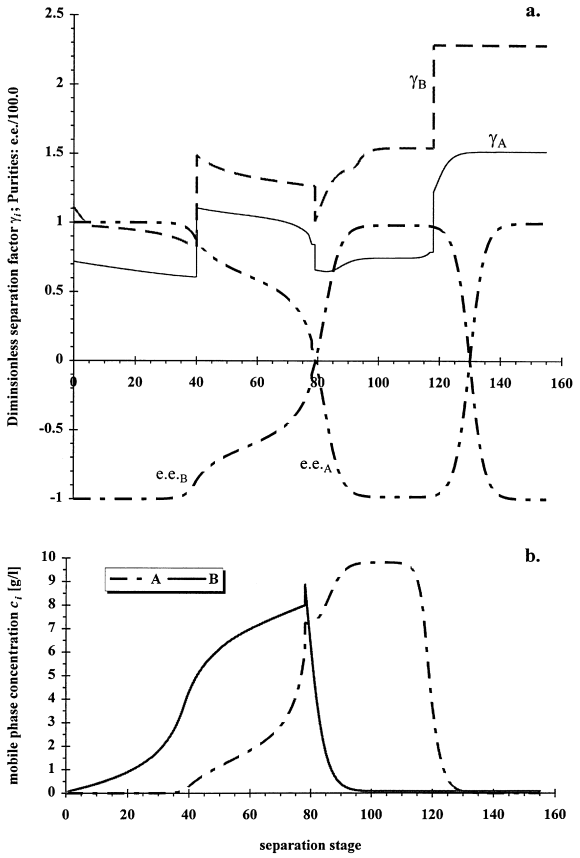

Fig. 8. (a) Dimensionless separation factor and purities for the optimized case. (b) Concentration profile within the SMB system.

Table 11
Comparison of the decision variables of run 03 and the optimal design

Run No.	$C_{i,\text{feed}}$ (g/l)	$\dot{V}'_{\text{feed}}$ (ml/min)	$\dot{V}'_{\text{L,I}}$ (ml/min)	$\dot{V}'_{\text{L,II}}$ (ml/min)	$\dot{V}'_{\text{L,III}}$ (ml/min)	$\dot{V}'_{\text{L,IV}}$ (ml/min)	$\dot{V}_S$ (ml/min)
03	10.0	0.40	3.84	2.64	3.04	2.24	0.51
Opt. Sim.	12.0	0.44	4.00	2.68	3.12	2.46	0.54

A concentration of $c_{feed} = 15$ g/l results in a raffinate e.e.$_A = 55\%$.

The experimental data represent the average of 1624 min (132 cycles) of operation. After the first two cycles a purity of e.e.$_{A,Ra} = 98\%$ and e.e.$_{B,Ex} = 97\%$ was obtained but the raffinate enantiomer excess dropped and reached the steady-state value given in Table 12. This result of an increase in J_1 of 1.77 mg/min or +24% compared to the best linear designed experiment was satisfactory. The achieved purities were sufficient because high enantiomerically pure antipodes could be obtained by a following crystallization step [24].

The remaining small deviations of simulation and experimental results of Table 12 may again be used for adapting the adsorption model. An additional iteration of the algorithms shown in Tables 5 and 3 would have to follow. This includes finding an adsorption model that fits the optimized run in addition to the four previously executed ones and updating the optimal design.

5. Conclusions

For utilizing the full potential of SMB technology it is necessary to operate the process under optimal conditions. Besides the feed concentration and feed flow-rate, four additional internal flow-rates need to be determined for a full specification of the process. It is a rather unrealistic approach trying to find the optimal setting to the operational specifications by repeated SMB experiments.

This paper gives a semi-deterministic two-step procedure which allows a quick and robust search for the optimal operating conditions. In the first step the six variables are determined by a Newton search method based on the free definition of an objective function. In a second step the adsorption isotherm model is corrected to match the SMB simulation with SMB experimental data.

By applying the proposed two-step procedure to the separation of a racemic mixture which shows nonlinear and coupled adsorption isotherms its robustness and efficiency could clearly be shown. The number of resource consuming SMB experiments can be kept at a minimum, which is considered to be the overall goal of the developed procedure. For comparison purposes the results for the straightforward linear approach in selecting the operational variables has been shown. No satisfactory result could be obtained by applying the classical linear adsorption model based approaches.

Additionally, the sensitivities of the individual operational variables on the purification power of the SMB system was investigated. Especially the solid flow-rate and the feed flow-rate – due to the nonlinear adsorption behavior of the system investigated – showed a strong dependency for the achieved purities and yields.

The proposed algorithm compacts deviations in the separation behavior of a SMB system in operation into the corrections of the adsorption isotherms only – including deviations such as changing flow patterns or variations in column packing. A tedious investigation for the cause becomes therefore obsolete and matching simulation results can still be provided.

6. Notation

6.1. Symbols

c	liquid phase concentration
$\mathbf{e}$	error vector
e.e.	enantiomer excess, e.e. $= (c_A - c_B)/(c_A + c_B)$
k	iteration variable
m	mth section number
q	solid-phase concentration
$\mathbf{s}$	search vector
t	retention time
t_0	zero retention time
u	solid-phase velocity
v	equivalent (true) liquid phase velocity
v'	actual liquid phase velocity
$\mathbf{y}$	decision variable vector
$\mathbf{y}^*$	optimal decision variable vector, $\mathbf{y}^* \equiv \min J$
A	column area
$\mathbf{H}$	Hessian matrix, $\mathbf{H} = \nabla^2 J$
J	objective function value
K	adsorption equilibrium constant, $K = q/c$
L	column length
M	amount of component collected

N	Nth separation stage
V_C	column volume, $V_C = AL$
$\dot{V}_L$	equivalent (true) liquid phase flow-rate
$\dot{V}'_L$	actual liquid phase flow-rate
$\dot{V}$	flow-rate

6.2. Greek letters

ε	total porosity
γ	dimensionless separation factor
τ	switching time
ξ	common factor for solving Eqs. (8)–(11)
Ω	weighing factor

6.3. Subscripts

feed	at feed stage
i	component I
l	extract or raffinate port
j	separation stage j
rec	recycle
s	solid-phase
A	component A
B	component B
Ex	extract stage
El	eluent (make-up)
L	liquid phase
Ra	raffinate stage
I to IV	section number

References

[1] D.B. Broughton, in Kirk-Othmer Encyclopedia of Chemical Technology, Vol. 1, Wiley, New York, 3rd ed., 1978.
[2] D.B. Broughton and S.A. Gembicki, in A.L. Myers and G. Belfort (Editors), Fundamentals of Adsorption, Engineering Foundation, New York, 1984.
[3] M.J. Gattuso and S. Makino, Simulated moving bed technology: a cost effective process for enantiomeric separations, presented at Chiral '94, Reston, VA, 1994.
[4] M. Negawa, F. Shoji, J. Chromatogr. 590 (1992) 113.
[5] C.B. Ching, B.G. Lin, E.J.D. Lee, S.C. Ng, J. Chromatogr. 634 (1993) 215.
[6] R.-M. Nicoud, G. Fuchs, P. Adam, M. Bailly, E. Küsters, F.D. Antia, R. Reuille, E. Schmid, Chirality 5 (1993) 267.
[7] E. Küsters, G. Gerber, F.D. Antia, Chromatographia 40 (1995) 387.
[8] D. Guest, J. Chromatogr. A 760 (1997) 159.
[9] E. Francotte and P. Richert, J. Chromatogr., (1997) in press
[10] C.B. Ching, D.M. Ruthven, Chem. Eng. Sci. 40 (1985) 877.
[11] C.B. Ching, D.M. Ruthven, Chem. Eng. Sci. 42 (1987) 2547.
[12] G. Ganetsos and P.E. Barker, in G. Ganetsos and P.E. Barker (Editors), Preparative and Production Scale Chromatography, Marcel Dekker, New York, 1993.
[13] C.B. Ching, C. Ho, D.M. Ruthven, Chem. Eng. Sci. 43 (1988) 703.
[14] D.M. Ruthven, C.B. Ching, Chem. Eng. Sci. 44 (1989) 1011.
[15] R.-M. Nicoud, LC·GC 5 (1992) 43.
[16] A.K. Ray, R.W. Carr, Chem. Eng. Sci. 50 (1995) 2195.
[17] K.H. Chu, M.A. Hashim, Chem. Eng. J. 56 (1995) 59.
[18] C.B. Ching, D.M. Ruthven, Chem. Eng. Sci. 41 (1986) 3063.
[19] A.E. Bryson and Y.C. Ho, Applied Optimal Control: Optimization, Estimation and Control, Hemisphere, New York, 1975.
[20] T.F. Edgar and D.M. Himmelblau, Optimization of Chemical Processes, McGraw-Hill, New York, 1988.
[21] T. Pröll, M.N. Karim, AIChE J. 40 (1994) 269.
[22] R.W. Rice and D.D. Do, Applied Mathematics and Modeling for Chemical Engineering, Wiley, New York, 1995.
[23] C. Roussel, J.-L. Stein, F. Beauvais, A. Chemlal, J. Chromatogr. 462 (1989) 95.
[24] E. Küsters, C.-P. Mak, B. Hildebrandt, B. Mutz, J. Therm. Anal. 41 (1994) 1183.